Synthesis, characterization and coordination chemistry of a new phosphite–ether ligand: The effects of alkali metal salts and the ligand/Rh molar ratio on the catalytic activity and regioselectivity of a Rh(I) complex of this ligand in the hydroformylation of styrene

Abha A. Kaisare [a], Samuel B. Owens Jr. [a], Edward J. Valente [b,1], Gary M. Gray [a,*]

[a] Department of Chemistry, University of Alabama at Birmingham, 901 14th Street South, Birmingham, AL 35294-1240, USA
[b] Department of Chemistry & Biochemistry, Mississippi College, 200 South Capitol Street, Clinton, MS 39056, USA

A R T I C L E   I N F O

A B S T R A C T

We have recently reported that the addition of alkali metal salts to styrene hydroformylation reactions catalyzed by Rh(I) complexes of bis(phosphite) ligands can significantly improve the iso/n regioselectivity. To better understand the effects of the alkali metal salts on these styrene hydroformylation reactions, a monodentate phosphite–ether ligand, $(2,2'-C_{12}H_8O_2)POCH_2CH_2OCH_3$, 1 has been prepared, and its Rh(I) complex has been evaluated as a catalyst for the hydroformylation of styrene. Both the activity and regioselectivity of the catalyst are sensitive to the ligand:Rh molar ratio and to the presence of salts such as $LiBPh_4 \cdot 3dme$, $NaBPh_4$ and $HgCl_2$. The most active catalyst has a 1:2.5 Rh:1 molar ratio and a 1:8 Rh:Li^+ molar ratio, but the most regioselective catalyst has a 1:8.2 Rh:1 ratio and a 1:4 Rh:Li^+ ratio. Model complexes for various steps in the catalytic cycle, cis-$Mo(CO)_4(\mathbf{1})_2$, **6**, cis-$PtCl_2(\mathbf{1})_2$, **7**, and $PdCl_2(\mathbf{1})_2$, **8**, have been synthesized and characterized by multinuclear NMR spectroscopy and X-ray crystallography to provide insight into the factors that may affect the rates and regioselectivities of the hydroformylation catalysts. The cis–$trans$ isomerization of **6** in the presence of catalytic amount $HgCl_2$ has been carried out to determine the cis–$trans$ preference of **1** in the octahedral coordination geometry.

© 2010 Elsevier B.V. All rights reserved.

1. Introduction

A wide variety of phosphorus-donor ligands have been evaluated in Rh catalysts for the hydroformylation of alkenes [1,2]. Among the most active and selective catalysts are Rh complexes of phosphite and bis(phosphite) ligands [3–5]. The phosphite and bis(phosphite) ligands are more resistant to oxidation [6] than are most of the other classes of phosphorus-donor ligands but are more weakly coordinating and degrade under catalytic reaction conditions [7].

Most studies have indicated that the major factor affecting the catalytic activities and regioselectivities of Rh complexes of phosphite and bis(phosphite) ligands is the steric bulk of the ligands. However, we have recently reported that the addition of a large excess of either $LiBPh_4 \cdot 3dme$ or $NaBPh_4$ to styrene hydroformylation reactions catalyzed either by a Rh(I) complex of (R,R)-Chiraphite® or by a Rh(I) metallacrown ether containing a tartaric acid-derived bis(phosphite)–polyether ligand, **2** (Fig. 1) significantly improves

the iso/n regioselectivity [8]. The effect of an alkali metal salt on the regioselectivity of styrene hydroformylations does not appear to be due to the increasing ionic strength of the solution because it is not linear with increasing salt concentration and it is not observed when the alkali metal salt is replaced with tetra-n-butyl-ammonium tetrafluoroborate [8].

These results suggest that the effect of an alkali metal salt on the regioselectivity of a styrene hydroformylations catalyzed by Rh(I) complexes of bis(phosphite) ligands could be due to cation binding to the carbonyl ligands [9–13]. It is unclear what role, if any, the bis(phosphite) ligands have in this cation binding. Cation binding to both transition metal complexes of simple phosphites [14] and functionalized bis(phosphites) (metallacrown ethers) [14,15] has been reported. However, the increases in the regioselectivity of the catalyst containing a bis(phosphite) functionalized with amide and ether binding sites (8%) was essentially the same as the increase in the regioselectivity for catalyst containing Chiraphite® with only phosphite functional groups [8].

To gain more insight into this effect, we have studied Rh(I) complexes of the monodentate phosphite polyether ligand $(2,2'-C_{12}H_8O_2)PO(CH_2CH_2OCH_3)$, **1** as a catalysts for the hydroformylation of styrene. Ligand **1** is similar to the bis(phosphite) ligands used in our previous study and in other studies of styrene

* Corresponding author. Tel.: +1 205 934 8094; fax: +1 205 934 2543.
  E-mail address: gmgray@uab.edu (G.M. Gray).
1 Present address: University of Portland, Swindells Hall, 5000 N Willamette Blvd., Portland, OR 97203, USA.
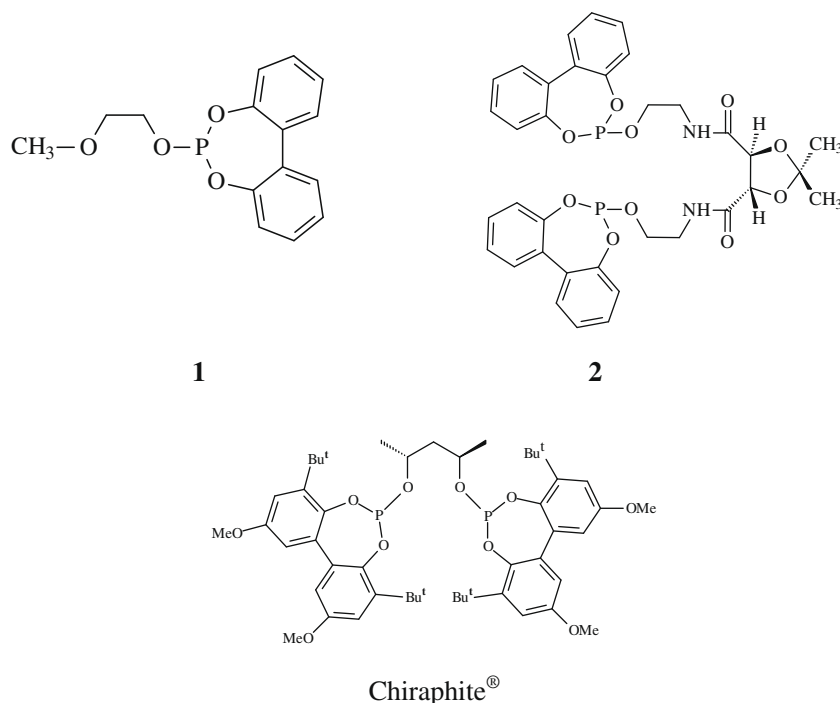
1

2

Chiraphite®

Fig. 1. Ligands used in the hydroformylation of styrene [8].

hydroformylation [16–22]. It is also similar to monodentate phosphite ligands [23–26] that have been used in Rh(I) catalysts for the hydroformylation of styrene and to phosphine/ether ligands that have been used in a variety of catalytic reactions such as alkene and CO_2 hydrogenation, alkene oligomerization and polymerization, methanol and methyl acetate carbonylation by Lindner et al. [27].

We have evaluated the catalytic activities and regioselectivies of Rh(I) complexes of **1** at three different ligand to Rh molar ratios in both the absence and presence of LiBPh₄·3dme, NaBPh₄ or HgCl₂ salts and these results are reported. We also report the synthesis and multinuclear NMR spectroscopic characterization of cis-Mo(CO)₄(**1**)₂, **6**, cis-PtCl₂(**1**)₂, **7**, and cis-PdCl₂(**1**)₂, **8**. Complex **6** is a model for octahedral intermediates in the catalytic cycle and allows cation binding by the octahedral intermediates and the coordination preferences of the phosphite ligand **1** in the octahedral intermediates to be evaluated. Complexes **7** and **8** are models for square-planar intermediates in the catalytic cycle and allow the coordination preferences of the phosphite ligand **1** in the square-planar intermediates to be evaluated. The X-ray crystal structures of **6** and **7** have been determined and provide insight into the potential conformations of the ligands in the octahedral and square-planar intermediates.

2. Experimental section

2.1. Materials and methods

All reactions and purification procedures were carried out under dry nitrogen. All starting materials were reagent grade and were used as received. Tetrahydrofuran (THF) was first distilled from calcium hydride and then from sodium/benzophenone and stored over molecular sieves. Triethylamine was distilled from sodium/benzophenone prior to use. 2-Methoxyethanol was dried by distillation from Mg/I₂ prior to use. Deuterated NMR solvents (chloroform-*d*, dichloromethane-*d₂*, acetonitrile-*d₃*) were opened and handled under a nitrogen atmosphere at all times.

LiBPh₄·3dme, NaBPh₄ and HgCl₂ were purchased from Aldrich and used as received. Literature procedures were used to prepare cis-Mo(CO)₄nbd, 2,2′-biphenylylenephosphochloridite ester, Rh(CO)₂- acac and PtCl₂(cod) [28–30].

All ³¹P{¹H}, ¹³C{¹H} and ¹H NMR spectra of the ligands and complexes were recorded using a Bruker DRX-400 NMR spectrometer. The ¹³C{¹H} and the ¹H NMR spectra were referenced to internal SiMe₄ while the ³¹P{¹H} NMR spectra were referenced to external 85% phosphoric acid. Quantitative ³¹P{¹H} NMR spectra were obtained with an inverse gated 30° pulse sequence and a delay of 10 s between pulses. Elemental analyses were performed by Atlantic Microlabs, Norcross, GA.

2.2. Synthesis of (2,2′-C₁₂H₈O₂)PO(CH₂CH₂OCH₃), 1

A solution of 2.07 mL (26.3 mmol) of 2-methoxyethanol, 6.58 g (26.3 mmol) of 2,2′-biphenylylenephosphochloridite ester and 3.64 mL (26.3 mmol) of triethylamine in 100 mL of freshly distilled THF was stirred under nitrogen for 12 h. The mixture was filtered through diatomaceous earth, and the filtrate was evaporated to dryness to yield 5.42 g (71.0%) of crude **1** as viscous, colorless oil. ³¹P{¹H} NMR (chloroform-*d*): δ 140.48 (s). ¹H NMR (chloroform-*d*): δ 3.40 (s, 3H, C*H₃*), δ 3.54 (t, 2H, |³*J*(HH)| 4.9 Hz, C*H₂*CH₂OP or C*H₂*OP), δ 4.08 (m, 2H, C*H₂*OP or C*H₂*CH₂OP), δ 7.19–7.47 (m, 8H, Ar*H*). ¹³C{¹H} NMR (chloroform-*d*): δ 150.28, (d, |²*J*(PC)| 5.4 Hz, Ar*C*O), 131.41 (d, |³*J*(PC)| 3.1 Hz, Ar*C*), 130.35 (bs Ar*C*H), δ 129.68 (bs Ar*C*H), 125.50 (s Ar*C*H), 122.38 (s, Ar*C*H), 72.45, (d, |²*J*(PC)| 3.7 Hz, *C*H₂OP), 64.11, (d, |³*J*(PC)| 4.6 Hz, *C*H₂CH₂OP), 59.44 (s, *C*H₃O).

2.3. Synthesis of cis-Mo(CO)₄{(2,2′-C₁₂H₈ O₂)PO(CH₂CH₂OCH₃)₂}, 6

A solution of 0.51 g (1.7 mmol) of Mo(CO)₄(nbd) and 1.0 g (3.4 mmol) of **1** in 200 mL of degassed dichloromethane was stirred for 2 h resulting in a pale yellow solution. This solution was evaporated to dryness, and the residue was washed with hexanes and then with methanol to yield 0.85 g (63%) of crude **6** as an off

white powder. The crude product was purified by recrystallization from a dichloromethane–hexanes mixture to give analytically pure **6** as colorless crystals. *Anal.* Calc. for $C_{36}H_{30}O_{12}P_2Mo$: C, 51.80; H, 3.83. Found: C, 51.92; H, 3.85%. $^{31}P\{^1H\}$ NMR (chloroform-*d*): δ 170.95 (s). ^1H NMR (chloroform-*d*): δ 3.29 (s, 3H, CH_3), 3.47 (t, 2H, $|^3J(HH)|$ 4.4 Hz, CH_2CH_2OP), 4.04 (m, 2H,CH_2OP), 7.24–7.48 (m, 8H, Ar*H*). $^{13}C\{^1H\}$ NMR (chloroform-*d*): δ 211.33 (*trans* CO aq, $|^2J(PC) + ^2J(PC')|$ 32.8 Hz), 206.59 (*cis* CO, t, $|^2J(PC)|$ 14.1 Hz), 149.82, (t, $|^2J(PC)|$ 4.6 Hz, Ar*C*O), 130.15 (s, Ar*C*), 130.03 (s Ar*C*H), 129.43 (s, Ar*C*H), 125.49 (s, Ar*C*H), 122.33 (s, Ar*C*H), 71.51, (t, $|^2J(PC)|$ 2.7 Hz, CH_2OP), 66.35, (t, $|^3J(PC)|$ 4.0 Hz, CH_2CH_2OP), 59.05 (s, CH_3O).

2.4. Synthesis of cis-PtCl₂{(2,2′-C₁₂H₈O₂)PO(CH₂CH₂OCH₃)₂}, 7

A solution of 0.40 g (1.1 mmol) of PtCl₂(cod) and 0.61 g (2.2 mmol) of **1** in 150 mL of degassed dichloromethane was stirred for 2 h, and then the solution was evaporated to dryness to yield 0.84 g (94%) of crude **7** as a white residue. The crude product was purified by recrystallization from a tetrahydrofuran–hexanes mixture to give analytically pure **7** as colorless crystals. *Anal.* Calc. for $C_{30}H_{30}O_8P_2Cl_2Pt$: C, 42.55; H, 3.54. Found: C, 42.71; H, 3.65%. $^{31}P\{^1H\}$ NMR (chloroform-*d*): δ 86.38 (s and d, $|^1J(PtP)|$ 5757.8 Hz). ^1H NMR (chloroform-*d*): δ 3.17 (s, 3H, CH_3), 3.41 (t, 2H, $|^3J(HH)|$ 3.7 Hz, CH_2OP), 4.29 (m, 2H CH_2, CH_2OP), 7.19–7.47 (m, 8H, Ar*H*). $^{13}C\{^1H\}$ NMR (chloroform-*d*) δ 148.01, (t, $|^2J(PC)|$ 5.0 Hz, Ar*C*O), 130.06 (s, Ar*C*), 129.85 (s, Ar*C*H), 129.210 (s, Ar*C*H), 126.66 (s Ar*C*H), 122.49 (bs Ar*C*H), 70.70, (t, $|^2J(PC)|$ 3.3 Hz, CH_2OP), 69.34, (s, CH_2CH_2OP), 58.78 (s, CH_3O).

2.5. Synthesis of PdCl₂{(2,2′-C₁₂H₈O₂)PO(CH₂CH₂OCH₃)₂}, 8

A mixture of 0.0036 g (0.020 mmol) of PdCl₂ in 0.25 mL of acetonitrile-*d₃* was stirred for 35 min to yield a light yellow solution of PdCl₂(CD₃CN)₂. The solution was then transferred into a 5 mm screw-top NMR tube containing 0.012 g (0.040 mmol) of **1** dissolved in 0.5 mL of acetonitrile-*d₃*. The solution was mixed for 10 min and then analyzed by NMR spectroscopy. $^{31}P\{^1H\}$ NMR (chloroform-*d*): δ 110.39 (s). ^1H NMR (chloroform-*d*): δ 3.08 (s, 3H, CH_3), 3.34 (m, 2H, CH_2O), 4.23 (m, 2H, CH_2OP), δ 7.31–7.52 (m, 8H, Ar*H*). $^{13}C\{^1H\}$ NMR (chloroform-*d*) δ 147.46, (bd, $|^2J(PC)|$ 4.8 Hz, Ar*C*O), δ 131.248 (s, Ar*C*), δ 129.94 (d $|^3J(PC)|$ 4.0 Hz, Ar*C*H), δ 128.65 (d $|^3J(PC)|$ 6.2 Hz, Ar*C*H), δ 126.77 (s Ar*C*H), δ 121.30 (s Ar*C*H), δ 70.08, (t, $|^2J(PC)|$ 3.4 Hz, CH_2OP) δ 69.43, (s, CH_2CH_2OP), δ 57.54 (s, CH_3O).

2.6. HgCl₂-catalyzed cis–trans isomerization of [cis-Mo(CO)₄{(2,2′-C₁₂H₈O₂)PO(CH₂CH₂OCH₃)₂}], 6

A solution of 0.0198 g (0.0250 mmol) of **6** in 0.5 ml of chloroform-*d* was prepared in a 5 mm, screw-top NMR tube under nitrogen, and the $^{31}P\{^1H\}$ NMR spectrum of the solution was recorded. Then, a catalytic amount of solid HgCl₂ was added to the solution. After 2 min of vigorous shaking, a $^{31}P\{^1H\}$ NMR spectrum was taken. Additional $^{31}P\{^1H\}$ NMR spectra were taken until the *cis:trans* ratio reached a constant value. Finally, a quantitative $^{31}P\{^1H\}$ NMR spectrum was taken. $^{31}P\{^1H\}$ NMR of mixture (chloroform-*d*): δ 170.95 (s, *cis* **6** isomer, 46.0%), 178.57 (s, *trans* **6** isomer, 54.0%).

2.7. X-ray structures of cis-Mo(CO)₄{(2,2′-C₁₂H₈O₂)PO(CH₂-CH₂OCH₃)₂}, 6 and cis-PtCl₂{(2,2′-C₁₂H₈O₂)PO(CH₂CH₂OCH₃)₂}, 7

A hot, saturated dichloromethane–hexanes solution of **6** and a hot, saturated tetrahydrofuran–hexanes solution of **7** were slowly cooled to yield X-ray quality, colorless, single crystals of each complex. A suitable crystal of **6** was attached to the tip of a 0.1 mm

diameter glass capillary and mounted on a goniometer head. The crystallographic properties and data were collected using Mo Kα radiation and the charge-coupled area detector (CCD) on an Oxford Diffraction Systems Gemini diffractometer at 104(2) K (1). A preliminary set of cell constants was calculated from reflections observed on three sets of five frames that were oriented approximately in mutually orthogonal directions of reciprocal space. Data collection was carried out using Mo Kα radiation (graphite monochromator) with nine runs consisting of 386 frames with a frame time of 15 s, and a crystal-to-CCD distance of 50.000 mm. The runs were collected by omega scans of 1.0° width, and at detector position 28.624° in 2θ. The intensity data were corrected for absorption. Final cell constants were calculated from 20 088 stronger reflections from the actual data collection after integration.

A suitable single crystal of **7** was glued on a glass fiber with epoxy and aligned on an Enraf Nonius CAD4 single crystal diffractometer under aerobic conditions. Standard peak search and automatic indexing routines followed by least-squares fits of 25 accurately centered reflections resulted in accurate unit cell parameters. The space group of the crystal was assigned on the basis of systematic absences and intensity statistics. Details of the data collection of each complex are given in Table 1. The analytical scattering factors of the complex were corrected for both $\Delta f'$ and

Table 1
Crystal structure data and refinement data for **6** and **7**.

	6	7
CCDC No.	692203	692422
Empirical formula	$C_{34}H_{30}O_8P_2Mo$	$C_{30}H_{30}Cl_2O_8P_2Pt$
Formula weight	788.46	846.47
Temperature (K)	104 (2)	293(2)
Wavelength (Å)	0.71073	0.71073
Crystal system	Monoclinic	Monoclinic
Space group	$P2_1/c$	$P2_1/c$
Unit cell dimensions		
a (Å)	14.8164 (4)	19.575(4)
b (Å)	10.6480(13)	9.5652(19)
c (Å)	21.3487(2)	19.493(4)
α (°)	90	90
β (°)	104.5182(12)	116.94(3)
γ (°)	90	90
Volume (Å³)	3260.55(11)	3253.6(11)
Z	4	4
Density (calculated) (Mg m⁻³)	1.606	1.728
Absorption coefficient (mm⁻¹)	0.567	4.622
F(0 0 0)	1608	1664
Crystal size (mm³)	$0.30 \times 0.30 \times 0.30$	$0.30 \times 0.46 \times 0.60$
Theta range for data collection (°)	3.02–30.60	2.09–22.48
Index ranges	$-19 \leqslant h \leqslant 21$, $-15 \leqslant k \leqslant 12$, $-30 \leqslant l \leqslant 30$	$-21 \leqslant h \leqslant 19$, $0 \leqslant k \leqslant 10$, $-1 \leqslant l \leqslant 20$
Reflections collected	26 922	4691
Independent reflections	9920 [R(int) = 0.0155]	4252 [R(int) = 0.0481]
Completeness to θ_{max} (°)	98.9%	100.0%
Absorption correction	Semi-empirical	Empirical
Maximum and minimum transmission	0.8484 and 0.8484	0.6974 and 0.5599
Refinement method	Full-matrix least-squares on F^2	Full-matrix least-squares on F^2
Data/restraints/parameters	9920/0/444	4252/0/390
Goodness-of-fit on F^2	1.056	0.988
Final R indices [$I > 2\sigma(I)$]	$R_1 = 0.0249$, $wR_2 = 0.0583$	$R_1 = 0.0409$, $wR_2 = 0.0956$
R indices (all data)	$R_1 = 0.0309$, $wR_2 = 0.1134$	$R_1 = 0.0939$, $wR_2 = 0.1134$
Largest difference peak and hole (e Å⁻³)	0.510 and −0.812	1.007 and −0.697

$i\Delta f''$ components of anomalous dispersion. All data were corrected for the effects of absorption and for Lorentz and polarization effects.

All crystallographic calculations were performed with the Siemens SHELXTL-PC program package [31]. The metal and P positions were located using the Patterson method and the remainder of the non-hydrogen atoms were located in difference Fourier maps. Full matrix refinement of the positional and anisotropic thermal parameters for all non-hydrogen atoms versus F^2 was carried out. All hydrogen atoms were placed in calculated positions with the appropriate molecular geometry and the $\delta(C–H) = 0.96$ Å. The isotropic thermal parameter associated with each hydrogen atom was fixed equal to 1.2 times the U_{eq} of the atom to which it was bound. Selected bond lengths, bond angles and torsion angles for complexes **6** through **7** are given in Table 2.

2.8. Hydroformylation of styrene

The catalysis reactions were carried out using a Parr Series 4560 minireactor connected to a high-pressure gas burette that introduced gas to the reactor at a constant pressure. The digitized reactor temperature, burette temperature, and burette pressure were monitored using Agilent Benchlink Data Logger software on a PC connected to an Agilent data acquisition switch unit. In a typical run, a solution of $Rh(CO)_2$acac and the alkali metal salt, if used, in 12 mL of dry THF and a solution of **1** in 10 mL of dry THF were separately added to the reactor via needle transfer under nitrogen pressure through the substrate inlet valve. The molar ratio of rhodium to phosphorus was varied for experiments to determine its effects on rate and selectivity. Next, the reactor was purged three times with a 1:1 H_2:CO gas (syngas) mixture and then pressurized to 20 atm with syngas and heated to 80 °C with mechanical stirring. The reactor was maintained under these conditions for 45 min to allow for pre-catalyst equilibration and then was cooled to 30 °C before the pressure was vented. Styrene (0.0337 mol) was then injected into the reactor through the substrate inlet valve, after which the reactor was pressurized to 20 atm with syngas and heated to 80 °C. The reaction progress was then monitored

using the Agilent software. The data obtained from pressure drop versus time were fitted to an exponential function using Graphical Analysis version 3.4 [32] to determine the pseudo-first order rate constant.

3. Results and discussion

### 3.1. Synthesis and NMR characterization of the monodentate phosphite/ether ligand, **1**

The ligand $(2,2'-C_{12}H_8O_2)PO(CH_2CH_2OCH_3)$ was prepared by the reaction of 2-methoxyethanol with 2,2'-biphenylylenephosphochloridite ester in THF in the presence of triethylamine (Scheme 1). The NMR spectra of **1** show no unexpected features. The chemical shift of the singlet $^{31}P\{^1H\}$ NMR resonance of the ligand was similar to those of others ligands with similar phosphorus environments [33,34]. The $^{13}C\{^1H\}$ NMR spectrum of the ligand exhibits well-resolved resonances for all of the methylene carbons. The resonances of the methylene carbons two and three bonds from the phosphorus (CH_2OP and CH_2CH_2OP, respectively) are doublets and are readily assigned by their chemical shifts and the relative values of the $|^nJ(PC)|$ coupling constants. The ^1H NMR spectrum of the ligand exhibits two resonances in the 3.54–4.08 ppm region, indicating that the protons attached to each methylene carbon are chemically equivalent. No attempt was made to assign these resonances. Because the $^{31}P\{^1H\}$, $^{13}C\{^1H\}$ and ^1H NMR spectra of the crude ligand contained no unexpected resonances, it was used in the syntheses of metal complexes and in the catalytic studies.

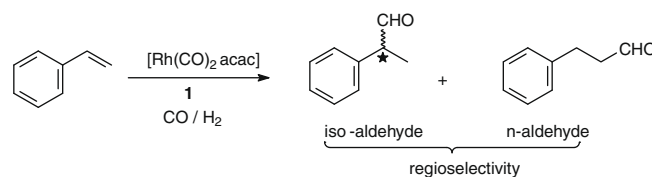### 3.2. Hydroformylation of styrene using ligand **1**

In the course of our investigations of the ability of a Rh(I) metallacrown ether containing a tartaric acid-based bis(phosphite)–polyether ligand to catalyze the hydroformylation of styrene [8], we found that the addition of $LiBPh_4\cdot3dme$ or $NaBPh_4$ improved the regioselectivity both of a Rh(I) catalyst containing this ligand and a Rh(I) catalyst containing Chiraphite® without affecting the rates of either reaction. To further explore the effects of alkali metal cations on styrene hydroformylation reactions, we have now evaluated *in situ* formed Rh(I) complexes of **1** (Scheme 2) as catalysts for the hydroformylation of styrene at three different ligand/Rh molar ratios in both the absence and presence of varying concentration of $LiBPh_4\cdot3dme$, $NaBPh_4$ or $HgCl_2$. Table 3 summarizes the experiments that were conducted. For each set of reaction conditions, two catalytic runs were carried out. The differences in the rate constants were less than 10% and differences in the % *iso* and % *n* were less than 2% for the duplicate runs.

Table 2
Selected bond lengths (Å), bond angles (°) and torsion angles (°) for **6** and **7**.

6		**7**	
P(1)–Mo	2.4291(3)	P(1)–Pt	2.189(3)
P(2)–Mo	2.4317(3)	P(2)–Pt	2.189(3)
C(31)–Mo	2.0241(14)	Cl(1)–Pt	2.333(3)
C(32)–Mo	2.0141(14)	Cl(2)–Pt	2.334(3)
C(33)–Mo	2.0430(14)		
C(34)–Mo	2.0405(15)		
C(31)–O(9)	1.1424(17)		
C(32)–O(10)	1.1452(17)		
C(33)–O(11)	1.1397(18)		
C(34)–O(12)	1.1410(19)		
P(1)–Mo–P(2)	96.207(11)	P(2)–Pt–P(1)	93.71(11)
C(31)–Mo–P(1)	171.46(4)	P(2)–Pt–Cl(1)	86.61(11)
C(32)–Mo–P(1)	86.27(4)	P(1)–Pt–Cl(1)	174.10(12)
C(33)–Mo–P(1)	93.69(4)	P(2)–Pt–Cl(2)	171.76(11)
C(34)–Mo–P(1)	85.06(4)	P(1)–Pt–Cl(2)	90.14(12)
C(31)–Mo–P(2)	87.70(4)	Cl(1)–Pt–Cl(2)	90.31(12)
C(32)–Mo–P(2)	171.55(4)		
C(33)–Mo–P(2)	87.36(4)		
C(34)–Mo–P(2)	93.00(4)		
O(1)–P(1)–Mo–P(2)	−86.82(5)	O(1)–P(2)–Pt–P(1)	−97.3(4)
O(4)–P(2)–Mo–P(1)	−10.98(5)	O(5)–P(1)–Pt–P(2)	−83.2(4)
C(19)–C(24)– C(25)–C(30)	39.68(19)	C(19)–C(24)–C(25)–C(30)	41.0(16)
C(7)–C(12)– C(13)–C(18)	47.24(18)	C(4)–C(9)– C(10)–C(15)	39.6(17)
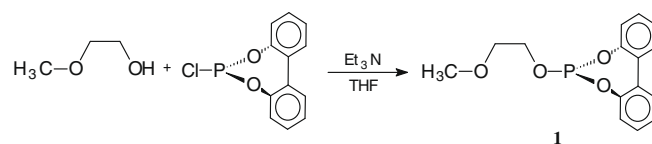
Scheme 1. Synthesis of ligand **1**.

Scheme 2. Hydroformylation of styrene using ligand **1**.

Table 3
Catalytic data for the hydroformylation of styrene using Rh(I) complexes of Ligand **1**.

Cation	k (s^{-1}) L/Rh = 1.5	k (s^{-1}) L/Rh = 2.5	k (s^{-1}) L/Rh = 8.2	% iso/% n L/Rh = 1.5	% iso/% n L/Rh = 2.5	% iso/% n L/Rh = 8.2
None	3.5×10^{-4}	3.5×10^{-4}	1.2×10^{-4}	76/24	75/25	85/15
1:1 LiBPh$_4$	3.0×10^{-4}			84/16		
2:1 LiBPh$_4$	2.9×10^{-4}			87/13		
4:1 LiBPh$_4$	2.9×10^{-4}	2.1×10^{-4}	8.7×10^{-5}	85/15	86/14	91/9
8:1 LiBPh$_4$	3.5×10^{-4}	6.7×10^{-4}	8.4×10^{-5}	85/15	86/14	89/11
32:1 LiBPh$_4$	3.4×10^{-4}	5.1×10^{-4}	7.2×10^{-5}	88/12	87/13	88/12
8:1 NaBPh$_4$		4.8×10^{-4}			87/13	
32:1 NaBPh$_4$	2.1×10^{-4}	4.5×10^{-4}	8.2×10^{-5}	89/11	87/13	89/11
1:1 HgCl$_2$	8.6×10^{-5}			68/32		

All numbers reported in this table are the average of those from two runs under identical conditions. Conditions (all ratios are molar): CO:H$_2$ = 1:1, T = 80 °C, P(CO/H$_2$) = 20 atm, substrate/Rh = 1000. Percentage conversion of styrene was greater than 99% in each case, and no hydrogenation of styrene was observed. The % iso/% n ratio was determined using ^{1}H NMR, and the differences in the % iso and % n were less than 2% for duplicate runs. The pseudo-first order rate constant (k) was obtained from a first-order fit of pressure drop vs. time using Graphical Analysis software [32], and the difference in the k values was less than 10% for duplicate runs.

The initial experiments were carried out with constant Rh and styrene concentrations while varying the ligand to Rh (L/Rh) ratio to determine the effect of the L/Rh ratio on the activity and regioselectivity of the catalyst. Neither the activity nor regioselectivity of the catalyst significantly changed when the L/Rh molar ratio was increased from 1.5:1 to 2.5:1 while the activity decreased by a factor of four and the iso:n ratio increased from 75:25 to 85:15 when the L/Rh molar ratio was increased to 8.2:1. These results suggest that the catalytically active species is the same for the lower L/Rh molar ratios but may change at the high L/Rh ratio. It seems likely that the active catalyst in each reaction is a Rh(I) complex of the phosphite ligand, **1**, rather than HRh(CO)$_4$ [35,36] because no hydrogenation of the alkene is observed at any of the L/Rh ratios [37–39]. The iso:n ratios are consistent with those expected for styrene, which has preference for the iso aldehyde [40], and are lower than those observed with Chiraphite® under the same reaction conditions (iso:n 91:9) [8].

The next experiments were carried out with constant Rh and styrene concentrations but with varying L/Rh and salt/Rh ratios to determine the effect of the salt on activity and regioselectivity of the catalyst. The most interesting results from this set of experiments are that the addition of LiBPh$_4$·3dme affected both the rate and regioselectivity of the hydroformylation reaction. The addition of 4:1 LiBPh$_4$·3dme to all of the reactions resulted in decreases in the reaction rates and increases in the iso:n ratios. In contrast, the addition of 8:1 LiBPh$_4$·3dme to the catalyst with L/Rh = 2.5:1 resulted in a 190% increase in the pseudo-first order rate constant and an increase in the iso:n ratio from 75:25 to 86:14. Addition of 32:1 of LiBPh$_4$·3dme to this catalyst had less of an effect on the rate (140% increase) and gave essentially the same iso:n ratio (87:13). The addition of either 8:1 or 32:1 LiBPh$_4$·3dme to the catalyst with L/Rh = 1.5:1 did not affect the pseudo-first order rate constant but had a similar effect on the iso:n ratio. Finally, the addition of LiBPh$_4$·3dme to the catalyst with L/Rh = 8.2 decreased the pseudo-first order rate constant with the decrease being proportional to the amount of salt that was added. As with the other catalysts, the addition of the LiBPh$_4$·3dme caused an increase in the iso:n ratio and this increase was relatively insensitive to the amount of salt that was added.

Other salts had somewhat different effects on the activities and regioselectivities of the catalysts. The addition of NaBPh$_4$ to the hydroformylation reactions affected both the activities and regioselectivities of the catalysts. As with LiBPh$_4$·3dme, the best rates were observed for the catalyst with L/Rh = 2.5:1 when 8:1 NaBPh$_4$ was used (140% increase). Increasing the NaBPh$_4$ to 32:1 did not significantly affect the regioselectivity of this catalyst. In contrast, the addition of 1:1 HgCl$_2$ to the catalyst with L/Rh = 1.5 caused a large decrease in the pseudo-first order rate constant. More interestingly, it also caused a larger decrease in the regioselectivity than

did the addition of 1:1 LiBPh$_4$·3dme. This demonstrates that the appropriate choice of hard metal salt allows the regioselectivity to be varied in either direction.

3.3. Syntheses and NMR characterizations of model complexes of **1**

Several model complexes have been synthesized and characterized to gain insight into the manner in which **1** coordinates to metals in octahedral and square planar coordination geometries similar to those that may be found in intermediates in the catalytic hydroformylation reaction. The model complexes also allow cation binding to the coordinated ligands in the complexes to be evaluated.

The cis-Mo(CO)$_4${(2,2′-C$_{12}$H$_8$O$_2$)PO(CH$_2$CH$_2$OCH$_3$)$_2$} **6** octahedral model complex was prepared as shown in Scheme 3. The single ^{31}P{^{1}H}NMR resonance of this complex at 170.95 ppm and the two well-resolved ^{13}C{^{1}H} resonances for the carbonyls in chloroform-d are consistent with the proposed structure for the complex. This complex is inert to ligand exchange, and the phosphite ligands occupy adjacent coordination sites that should be optimal for cation binding. In spite of this, the position of the ^{31}P{^{1}H} NMR resonance does not appreciably change when a 55-fold excess of LiBPh$_4$·3dme is added to the dichloromethane-d_2 solution. This suggests that the complex is, at best, a weak binder of Li$^+$ cations in dichloromethane-d_2 solution.
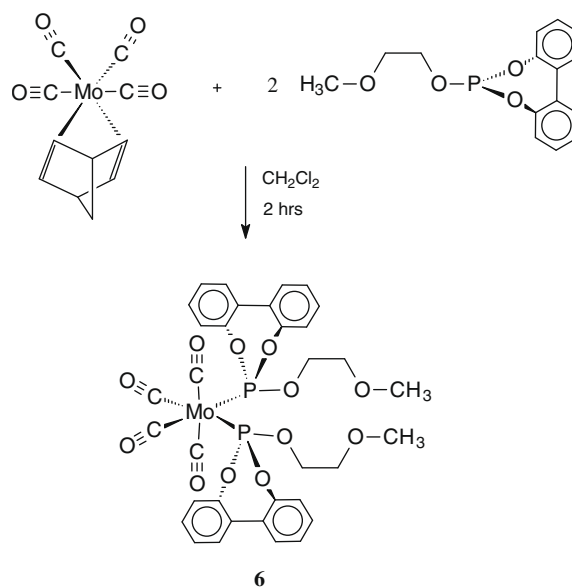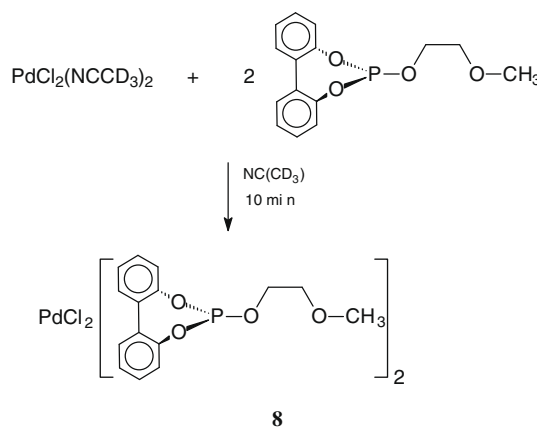

Scheme 3. Synthesis of complex **6**.
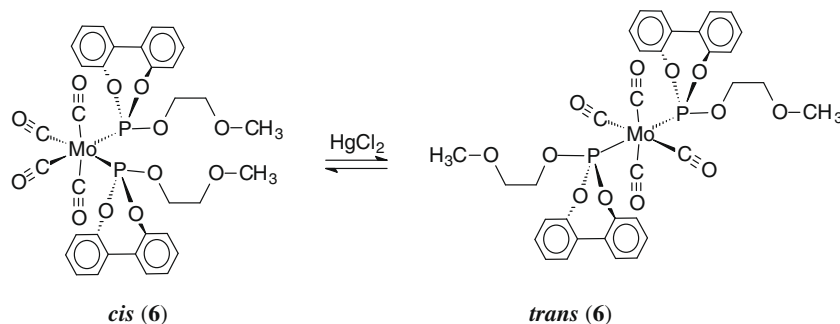
Scheme 4. HgCl$_2$-catalyzed *cis–trans* isomerization of complex **6**.

To better understand the coordination preferences of the phosphite ligands, the HgCl$_2$-catalyzed *cis–trans* isomerization of **6**, shown in Scheme 4, was followed by ^{31}P{^{1}H} NMR spectroscopy to determine the *cis–trans* preference of **1** in an octahedral complex. At equilibrium, the *cis:trans* ratio was 46:54 indicating that the ligand does not have a significant preference for either isomer.

The *cis*-PtCl$_2${(2,2′-C$_{12}$H$_8$O$_2$)PO(CH$_2$CH$_2$OCH$_3$)$_2$} **7** square planar model complex was prepared as shown in Scheme 5. The single ^{31}P{^{1}H} NMR resonance of this complex and the magnitude of the one bond Pt–P coupling constant indicate that a single geometrical isomer with the two phosphite ligands *cis* to one another is present.

The PdCl$_2${(2,2′-C$_{12}$H$_8$O$_2$)PO(CH$_2$CH$_2$OCH$_3$)$_2$} **8** square planar model complex was prepared as shown in Scheme 6. Surprisingly, the ^{31}P{^{1}H} NMR spectrum of the complex in chloroform-*d* exhibited a single singlet resonance indicating that only one geometrical isomer was present in the solution. Unfortunately, it was not possible to determine which of the geometrical isomers is present based solely on the chemical shift of the ^{31}P{^{1}H} NMR resonance, and the complex was also insufficiently stable in solution to allow X-ray quality single crystals to be obtained.

This result is surprising because, as indicated above, both the *cis* and *trans* isomers of the octahedral model complex, **6**, were observed at equilibrium. In addition, closely related PdCl$_2${Ph$_2$P(CH$_2$-CH$_2$O)$_n$CH$_2$CH$_2$PPh$_2$} (*n* = 3, 4, 5) metallacrown ethers exhibit both *cis* and *trans* geometrical isomers of both monomeric and cyclic
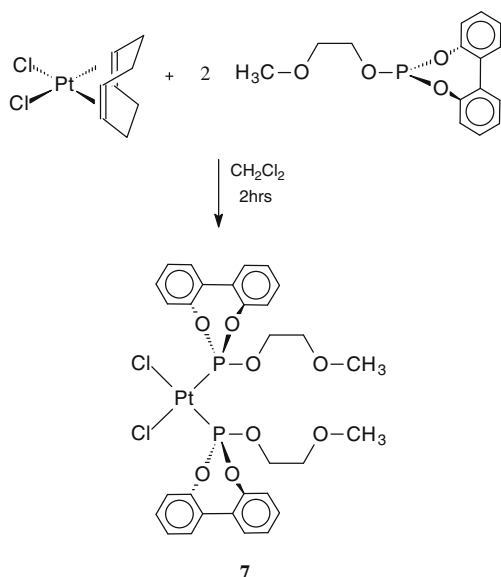

Scheme 6. Synthesis of complex **8**.

oligomeric complexes at equilibrium [41,42]. These results suggest that coordination preferences of the ligands may be affected by the nature of phosphorus-donor group in the ligand, the nature of the *trans* ligands (π-acceptor carbonyls in **6** versus π-donor chlorides in **7**) and/or the coordination environment about the metal (octahedral in **6** versus square planar in **7**). These preferences could be directly related to the catalytic results because it is well established that the equatorial–equatorial or equatorial–apical preferences of bis(phosphite) ligands have significant effects on the regioselectivities of their Rh(I) hydroformylation catalysts [43].

3.4. X-ray crystal structures of the model complexes **6** and **7**

The X-ray crystal structures of **6** and **7** have been determined, and the molecular structures are shown in Figs. 2 and 3, respectively. These structures are of interest because they allow the effect of the coordination environment of the metal center on the ligand to be examined and because they are closely related to the previously reported structures of sterically unhindered and symmetrical metallacrown ethers [44–48].

Consistent with the NMR data, **6** has a *cis* octahedral coordination geometry similar to that seen in other *cis*-Mo(CO)$_4$(P-donor ligand)$_2$ complexes [45,46]. The octahedron is significantly distorted as indicated by the deviation of the phosphorus–molybdenum–phosphorus bond angle (96.21(11)°) from the ideal angle of 90°. The coordination geometry of the platinum in **7** is a distorted square plane composed of two *cis* chlorines and two *cis* phosphites similar to that observed in other *cis*-PtCl$_2$(P-donor ligand)$_2$ complexes [47,48]. The distortion in the phosphorus–platinum–phosphorus angle (93.71(11)°) is significantly less than in the phosphorus–molybdenum–phosphorus bond angle suggesting perhaps that the square planar coordination geometry in **7** allows for reduced steric interactions between the two phosphite ligands.
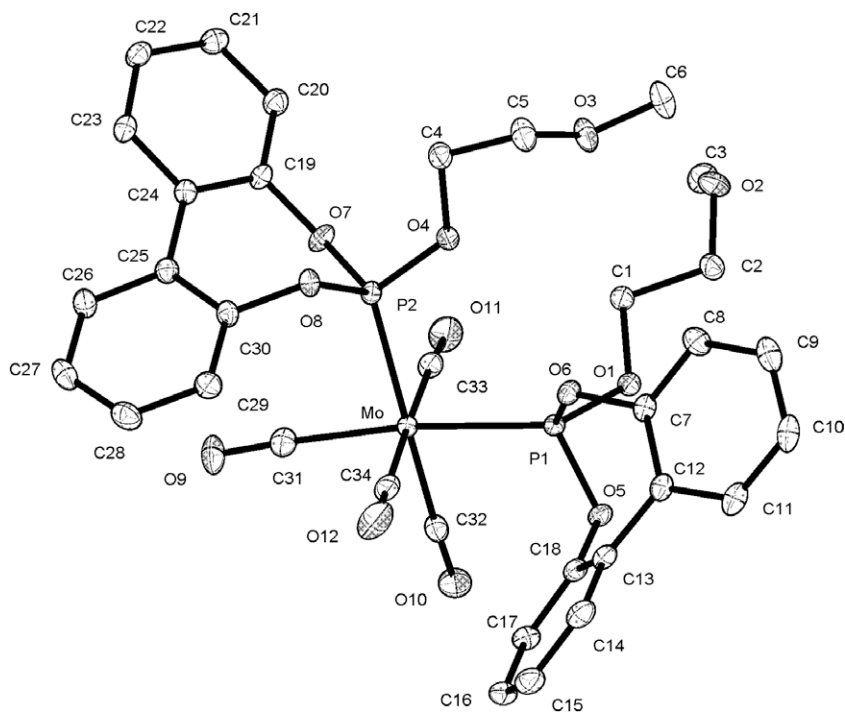

Scheme 5. Synthesis of complex **7**.

Fig. 2. ORTEP drawing of the molecular structure of **6**. The hydrogens are omitted for clarity, and the thermal ellipsoids are drawn at the 50% probability level.

Fig. 3. ORTEP drawing of the molecular structure of **7**. The hydrogens are omitted for clarity, and the thermal ellipsoids are drawn at the 50% probability level.
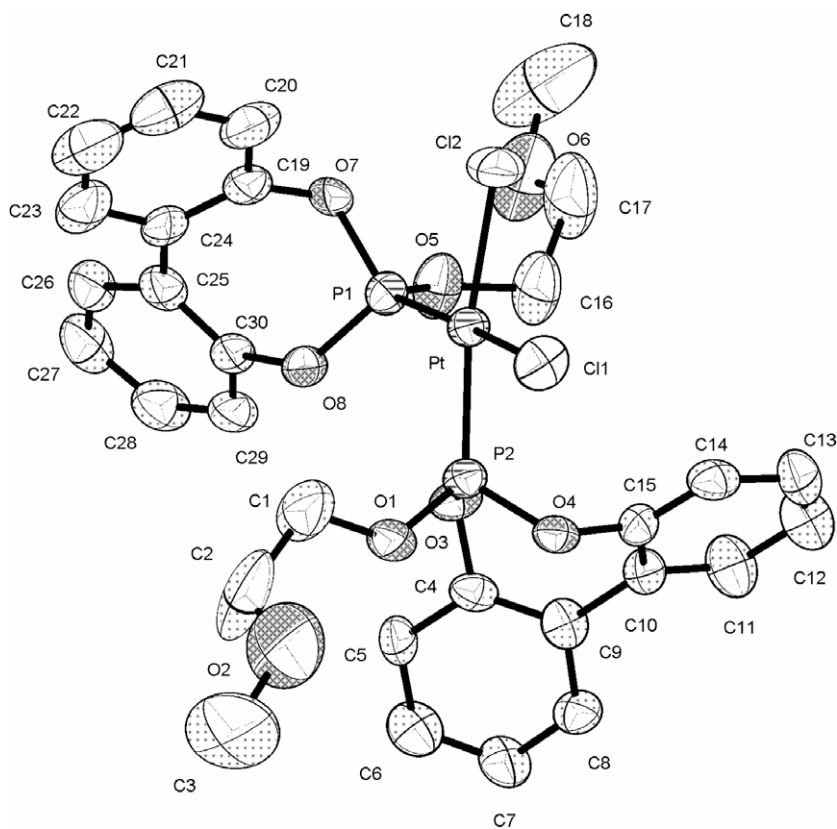
The most interesting feature of structures of **6** and **7** is relative orientation of the two ligands as described by the torsion angles about the Mo–P bonds given in Table 2. These torsion angles are similar in the two complexes and indicate that one of the P–O bonds is nearly in the plane formed by the metal, P1 and P2 while the other is nearly perpendicular to this plane. This is apparently

due to the steric constraints imposed by crystal packing forces because the NMR spectroscopic studies indicate that the two chains are equivalent in solution.

Another interesting feature of the molecular structures of **6** and **7** is the conformation of the biphenyl rings. These conformations are defined by the torsion angles about the bonds between the two phenylene rings and, as shown in Table 2, these angles are very similar. This is consistent with previous results that indicate that the phosphepin rings have a strongly preferred conformation that is not significantly affected by either crystal packing forces or by orientation of the phosphite ligands relative to the metal center [49].

4. Conclusions

Rhodium(I) complexes of the phosphite/ether ligand **1** are active catalysts for the hydroformylation of styrene. The use of high L/Rh ratios results in lower activities and higher regioselectivities but varying the L/Rh ratio between 1.5:1 and 2.5:1 does not affect either the activity or regioselectivity of the catalyst. The addition of either $LiBPh_4 \cdot 3dme$ or $NaBPh_4$ to the catalytic reactions can affect both the activity and the regioselectivity depending on the L/Rh ratio and the amount of the salt that is used. The best activities are observed with catalysts with L/Rh = 2.5:1 and 8:1 $LiBPh_4 \cdot 3dme$ while the regioselectivities remain relatively constant at salt/Rh ratios of 4:1–32:1. These results suggest that it may be possible to optimize both the reaction rate and regioselectivity by the appropriate choice of ligand, L/Rh ratio, amount and type of alkali metal salt that is added to the reaction mixture.

We have previously hypothesized that alkali metal salts could positively affect the activities of hydroformylations catalyzed by bis(phosphite) complexes of Rh(I) result from cation binding to the carbonyl oxygen of either a carbonyl or acyl ligand [8]. Such binding is known to activate carbonyl ligands towards nucleophilic attack and to weaken the metal–carbonyl bond [9–14], which would facilitate migratory-insertion reactions [50,51] in the catalytic cycle and could also affect the equilibria between five-coordinate reservoir species and four-coordinate active intermediates for the alkene coordination and H_2 oxidative-addition steps in the catalytic cycle. The results from this study with catalysts having L/Rh = 2.5 are consistent with this hypothesis.

Appendix A. Supplementary material

CCDC 692203 and 692422 contain the supplementary crystallographic data for complexes **6** and **7**. These data can be obtained free of charge from The Cambridge Crystallographic Data Centre via www.ccdc.cam.ac.uk/data_request/cif. Supplementary data associated with this article can be found, in the online version, at doi:10.1016/j.jorganchem.2010.03.001.

References

[1] A.T. Axtell, J. Klosin, G.T. Whiteker, C.J. Cobley, M.E. Fox, M. Jackson, K.A. Abboud, Organometallics 28 (2009) 2993.
[2] Y. Guo, H. Fu, H. Chen, X. Li, Catal. Commun. 9 (2008) 1842.
[3] A.A. Dabbawala, H.C. Bajaj, R.V. Jasra, J. Mol. Catal. A: Chem. 302 (2009) 97.
[4] A. Gual, C. Godard, C. Claver, S. Castillon, Eur. J. Org. Chem. 8 (2009) 1191.
[5] J. Tijani, B. El Ali, J. Organomet. Chem. 692 (2007) 3492.
[6] G.J.H. Buisman, M.E. Martin, E.J. Vos, A. Klootwijk, P.C.J. Kamer, P.W.N.M. Van Leeuwen, Tetrahedron: Asymmetry 6 (1995) 719.
[7] P.W.N.M. Van Leeuwen, C. Claver, Rhodium Catalyzed Hydroformylation, Kluwer Academic Publishers, New York, 2000. p. 35.
[8] S.B. Owens Jr., G.M. Gray, Organometallics 27 (2008) 4282.
[9] J. Powell, M.R. Gregg, A. Kuksis, C.J. May, S.J. Smith, Organometallics 8 (1989) 2918.
[10] J. Powell, M.R. Gregg, P.E. Meindl, Organometallics 8 (1989) 2942.
[11] J. Powell, A. Lough, F. Wang, Organometallics 11 (1992) 2289.
[12] J. Powell, M.R. Gregg, A. Kuksis, C.J. May, J. Am. Chem. Soc. 103 (1981) 5941.
[13] J. Powell, M. Gregg, A. Kuksis, P.E. Meindl, J. Am. Chem. Soc. 105 (1983) 1064.
[14] J. Powell, A. Kuksis, C.J. May, P.E. Meindl, S.J. Smith, Organometallics 8 (1989) 2933 (See Eq. (8) and Fig. 3c on page 2937 for simple phosphites).
[15] J.M. Butler, M.J. Jablonsky, G.M. Gray, Organometallics 22 (2003) 1081.
[16] A. van Rooy, P.C.J. Kamer, P.W.N.M. van Leeuwen, K. Goubitz, J. Fraanje, N. Veldman, A.L. Spek, Organometallics 15 (1996) 835.
[17] G. Erre, S. Enthaler, K. Junge, S. Gladiali, M. Beller, J. Mol. Catal. A: Chem. 280 (2008) 148.
[18] A.T. Axtell, J. Klosin, K.A. Abboud, Organometallics 25 (2006) 5003.
[19] T.P. Clark, C.R. Landis, S.L. Freed, J. Klosin, K.A. Abboud, J. Am. Chem. Soc. 127 (2005) 5040.
[20] A.T. Axtell, C.J. Cobley, J. Klosin, G.T. Whiteker, A. Zanotti-Gerosa, K.A. Abboud, Angew. Chem., Int. Ed. 44 (2005) 5834.
[21] K. Nozaki, N. Sakai, T. Nanno, T. Higashijima, S. Mano, T. Horiuchi, H. Takaya, J. Am. Chem. Soc. 119 (1997) 4413.
[22] C.B. Dieleman, P.C.J. Kamer, J.N.H. Reek, P.W.N.M. Van Leeuwen, Helvetica Chim. Acta 84 (2001) 3269. and refereces therein.
[23] A. van Rooy, E.N. Orij, P.C.J. Kamer, P.W.N.M. van Leeuwen, Organometallics 14 (1995) 34.
[24] M.T. Reetz, X. Li, Angew. Chem., Int. Ed. 44 (2005) 2962.
[25] T. Jongsma, G. Challa, P.W.N.M. van Leeuwen, J. Organomet. Chem. 421 (1991) 121.
[26] J. Klosin, C.R. Landis, Acc. Chem. Res. 40 (2007) 1251.
[27] E. Lindner, S. Pautz, M. Haustein, Coord. Chem. Rev. 155 (1996) 145.
[28] L.V. Verizhnikov, P.A. Kirpichnikov, Zh. Obshch. Khim. 37 (1967) 1355.
[29] W. Ehrl, R. Rinck, H. Vahrenkamp, J. Organomet. Chem. 56 (1973) 285.
[30] Y.S. Varshavskii, T.G. Cherkasova, Zh. Obshch. Khim. 12 (1967) 1709.
[31] G.M. Sheldrick, SHELXTL NT ver. 5.10, Brucker AXS, Inc., Madison, WI, 1999.
[32] Graphical Analysis, 3.4, Vernier Software and Technology, Beaverton, OR, 2005.
[33] J.G. Verkade, L.D. Qiun, Phosphorus-31 NMR Spectroscopy in Stereochemical Analysis: Organic Compounds and Metal complexes, VCH, Weinheim, 1987.
[34] M. Hariharasarma, G.M. Gray, J. Organomet. Chem. 580 (1999) 328.
[35] G. Liu, R. Volken, M. Garland, Organometallics 18 (1999) 3429.
[36] J. Feng, M. Garland, Organometallics 18 (1999) 417.
[37] J.P. Collman, L.S. Hegedus, J.R. Norton, R.G. Finke, Principles and Applications of Organotransition Metal Chemistry, University Science Books, Mill Valley, CA, 1987. p. 625.
[38] J.L. Vidal, W.E. Walker, Inorg. Chem. 20 (1981) 249.
[39] B.R. James, Homogeneous Hydrogenation, Wiley-Interscience, New York, 1973. p. 263.
[40] P.W.N.M. Van Leeuwen, Homogeneous Catalysis: Understanding the Art, Kluwer Academic Publishers, MA, 2004. p. 166.
[41] D.C. Smith Jr., G.M. Gray, Inorg. Chem. 37 (1998) 1791.
[42] D.C. Smith Jr., C.H. Lake, G.M. Gray, Chem. Commun. 24 (1998) 2771.
[43] A. van Rooy, P.C.J. Kamer, P.W.N.M. van Leeuwen, N. Veldman, A.L. Spek, J. Organomet. Chem. 494 (1995) C15.
[44] G.M. Gray, F.P. Fish, C.H. Duffey, Inorg. Chim. Acta 261 (1997) 233.
[45] C.H. Duffey, C.H. Lake, G.M. Gray, Inorg. Chim. Acta. 317 (2001) 199.
[46] C.H. Duffey, C.H. Lake, G.M. Gray, Organometallics 17 (1998) 3550.
[47] A. Varshney, M.L. Webster, G.M. Gray, Inorg. Chem. 31 (1992) 2580.
[48] A. Varshney, G.M. Gray, Inorg. Chem. 30 (1991) 1748.
[49] H. Byrd, J.D. Harden, J.M. Butler, M.J. Jablonsky, G.M. Gray, Organometallics 22 (2003) 4198.
[50] S.B. Butts, S.H. Strauss, E.M. Holt, R.E. Stimson, N.W. Alcock, D.F. Shriver, J. Am. Chem. Soc. 102 (1980) 5093.
[51] T.G. Richmond, F. Basolo, D.F. Shriver, Inorg. Chem. 21 (1982) 1272.